Science of the Total Environment 954 (2024) 176600

Contents lists available at ScienceDirect

Science of the Total Environment

journal homepage: www.elsevier.com/locate/scitotenv

In-depth analysis of natural organic matter fractions in drinking water treatment performance: Fate and role of humic substances in trihalomethanes formation potential

Meritxell Valenti-Quiroga [a], Alba Cabrera-Codony [a], Pere Emiliano [b], Fernando Valero [b], Hèctor Monclús [a], Maria J. Martin [a,*]

[a] LEQUIA, Institute of the Environment, Universitat de Girona, Carrer Maria Aurèlia Capmany, 69, E-17003 Girona, Spain
[b] Ens d'Abastament d'Aigua Ter-Llobregat (ATL), Sant Martí de l'Erm 2, E-08970 Sant Joan Despí, Barcelona, Spain

HIGHLIGHTS

- HPSEC-DAD-OCD revealed HS1 as the most abundant and aromatic sub-fraction.
- Conventional treatments targeted higher MW DOM, while EDR and IEX focused on lower MW.
- Spectroscopic analysis identified key absorbance features linked to DBP precursors.
- Absorbance ratios highlighted differences in aromaticity and polarity across DOM.
- Distinct THM speciation in river vs. reservoir water influenced by bromide presence

GRAPHICAL ABSTRACT

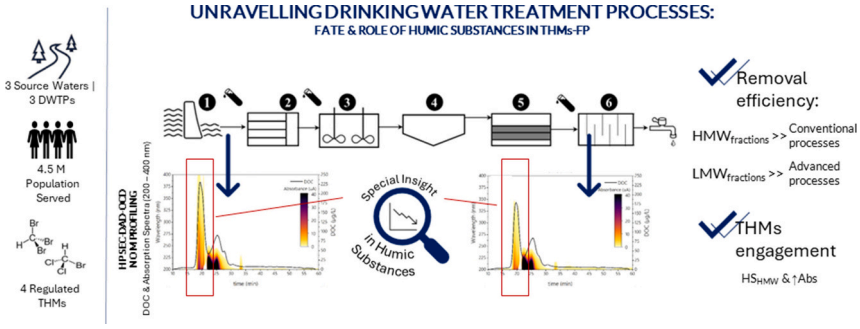

ARTICLE INFO

Editor: Damia Barcelo

Keywords:
Dissolved organic matter (DOM)
Disinfection by-products (DBPs)
High performance size exclusion chromatography (HPSEC)
Humic substances
UV-absorbance

ABSTRACT

In this study we investigate the compositional changes in dissolved organic matter (DOM) fractions across diverse water sources and treatment processes in three Drinking Water Treatment Plants (DWTPs). High-Performance Size Exclusion Chromatography coupled with Diode Array Detection and Organic Carbon Detection (HPSEC-DAD-OCD) was employed to characterize DOM fractions, offering insights into treatment optimization. We examine bulk water parameters, DOM distributions, and the efficiency of treatment trains in reducing DOM fractions. Results reveal distinct DOM composition profiles in river-sourced versus reservoir-sourced waters, with implications for treatment processes. Coagulation, Granular Activated Carbon (GAC) adsorption, Electrodialysis Reversal (EDR), and Ion Exchange (IEX) were evaluated for their efficacy in removing DOM fractions. The analysis highlights the effectiveness of coagulation in reducing high molecular weight (MW) fractions, while GAC filtration targets lower MW fractions. EDR shows significant removal of anions and aromatics, while IEX demonstrates high removal efficiencies for removing humic substances (HS) fractions. Spectroscopic analysis further elucidates changes HS sub-fractions and their role in disinfection by-products (DBP) formation. To quantitatively assess the relationship between HS sub-fractions and trihalomethane formation

* Corresponding author.
E-mail address: maria.martin@udg.edu (M.J. Martin).

https://doi.org/10.1016/j.scitotenv.2024.176600
Received 17 June 2024; Received in revised form 24 September 2024; Accepted 27 September 2024
Available online 28 September 2024

potentials (THMFP), Pearson correlation analysis were conducted, unveiling robust associations between HS sub-fractions and THM-FP that can be predicted by surrogate parameters such as A_{254}.

1. Introduction

Dissolved organic matter (DOM) is a heterogeneous complex mixture of organic compounds found in drinking water sources. Its composition depends on the water source, its quality and quantity, as well as the seasonality and environmental changes, which add complexity to the drinking water treatment plants (DWTPs) operation. Because the presence of unremoved DOM contributes to the formation of toxic disinfection by-products (DBPs) upon chlorination, its removal before the final disinfection stage is crucial to prevent an increase in DBPs concentrations and a highly challenging task due to its complex composition.

The research conducted over the past decades has proven that hydrophobic and high molecular weight (HMW) compounds, which contain large amounts of aromatic carbons, are the main precursors of DBPs formation (Awad et al., 2016; Korshin et al., 2002), while hydrophilic and low molecular weight (LMW) compounds can also contribute (Andersson et al., 2020; Bond et al., 2009; Finkbeiner et al., 2020). Non-aromatic DOC components, such as protein-like compounds, although contributing to a lesser extent than humic substances, are also important precursors of THMFP and should not be excluded from consideration (Abouleish and Wells, 2015). However, the formation of DBPs is not solely influenced by of organic compounds, but also by inorganic anions such as bromide and iodine, which react differently: while chlorine shows higher reactivity towards hydrophobic HMW compounds, bigger halogens appear to be more reactive with LMW hydrophilic fractions (Valenti et al., 2022). Thus, it becomes paramount to understand the role and fate of the principal components of DOM, since optimizing water treatment for the abatement of both categories of compounds is crucial in mitigating DBPs formation.

Coagulation is the most widely used process for DOM removal due to its cost-benefit balance. During this process, small aggregates are formed through the brownian motion after the addition of iron or aluminium salts that destabilizes the suspended solids and colloidal matter. Subsequently, flocculation occurs, leading to the formation of large flocs that are further separated by sedimentation. After the coagulation/flocculation stage that eliminates mainly HMW compounds, granular activated carbon (GAC) filtration is typically used to adsorb mid and low molecular weight compounds (Valverde et al., 2024), with hydrophobic fractions being selectively removed over the hydrophilic ones (Bhatnagar and Sillanpää, 2017; Velten et al., 2011). Ion exchange processes (IEX) are an alternative to conventional treatments for DOM removal (Drikas et al., 2011; Finkbeiner et al., 2018), consisting of the reversible exchange of ions between the water and the solid phase resin driven by electrostatic interactions with the functional groups and physical adsorption of hydrophobic moieties by Van der Waals interactions (Tan and Kilduff, 2007).

The need for a methodology capable of tracking subtle changes in DOM during water treatment processes and predicting subsequent DBP generation is evident, given the varied impact of treatments on overall DOM removal. While literature often focuses on evaluating spectroscopic changes at 254 nm, which correlate with conjugated double bonds and aromatic structures, (Peacock et al., 2014) found that single absorbance measurements at 230 nm and 263 nm can serve as proxies for DOC. However, (Awad et al., 2016) reported that monitoring general parameters such as DOC proxies in presence of bromide alone may not be sufficient to understand the reactivity of DOM towards DBP formation.

In this context, integrating a field-deployable UV-VIS methodology offers a cost-efficient means to monitor temporal changes (Chen et al., 2020; Chen and Yu, 2021; Rodríguez et al., 2016). Multiwavelength sensors can create robust databases and minimize random errors, unlike single wavelength measurements (Korshin et al., 2002; Roccaro et al., 2009). According to Lambert-Beer law, absorbance is proportional to the concentration of chromophores, a property that applies to mixtures as far as no reaction is involved. In such cases, the overall absorbance (area under the full UV-spectra) is equal to the sum of the contributions from all the present compounds. Therefore, information from other previously used proxies, such as specific wavelengths, differential absorbance, or ratios, are embedded in a single measurement. Moreover, a multiwavelength determination can reduce the random error associated to single wavelength monitoring, which is caused by strong dependence on a major functionality or fraction. This reinforces the potential of monitoring characteristic DOM alterations by the multiwavelength ranges analysis, in accordance with (Wang and Hsieh, 2001) who emphasized that monitoring between spectroscopic ranks could minimize random error of single measurements and also provides wider information from the diverse constituting functionalities. However, interpreting bulk determinations can be challenging due to the inability to discern absorbance attributed to specific DOM constituents or separate signals from interfering compounds like inorganics (Shi et al., 2022; Wang and Hsieh, 2001).

High-Performance Size Exclusion Chromatography (HPSEC) emerges as a suitable technique for providing additional information based on molecular weight (MW) separation, effectively eliminating interferences such as inorganic ions (Cascone et al., 2022; Yan et al., 2012). The combination of a diode array detector (DAD) coupled to an organic carbon detector (OCD) after the chromatography (HPSEC-DAD-OCD), enables depicting absorbance related to the carbon content of each DOM fraction. This yields a characteristic fingerprint that can ease understanding the physicochemical properties of DOM constituents. Evaluating the spectroscopic changes in fractionated samples using HPSEC-DAD-OCD provides a better understanding on the nature of DOM constituents, highlights the site-specificity of water matrices, and contributes to understand their behavior against treatments, including their impact on the formation of THM.

Although HPSEC-DAD-OCD provides valuable information, there is limited research exploring correlations between HPSEC fractions and the formation of disinfection by-products (DBPs), particularly with a multiwavelength monitoring approach (Brezinski and Gorczyca, 2019; Valenti et al., 2022). This study aims to bridge this gap by investigating the compositional changes in DOM fractions across diverse water sources and treatment processes in three Drinking Water Treatment Plants (DWTPs). River-sourced and reservoir-sourced waters exhibit distinct DOM composition profiles due to differences in catchment characteristics, land use, and hydrological regimes (Gibert et al., 2013). The efficiency of treatment trains, including conventional processes at full scale (coagulation/flocculation, GAC adsorption, disinfection) and advanced operations in full (EDR) and bench scale (IEX), in removing DOM fractions is evaluated to assess the suitability of different treatment technologies for mitigating organic contaminants (Carra et al., 2021). Furthermore, spectroscopic analysis is employed to elucidate changes in humic substances (HS) sub-fractions and their implications for DBP formation during chlorination. By correlating DOM composition with water quality parameters, this study aims to provide valuable insights into the optimization of water treatment processes and the management of organic contaminants in drinking water supplies.

Through a comprehensive analysis of the impact of sequential treatment operations on the distribution of DOM fractions and their relation to the decrease in trihalomethanes formation potential (THMFP), this study explores absorbance changes in the full UV spectra (from 200 nm to 400 nm). It constitutes a step forward towards

elucidating the correlation between fractionated and bulk wavelength measurements, which is essential for implementing multiwavelength UV sensors for real-time monitoring, facilitating operational management and the optimization of processes to maximize THM precursors according to the specific composition of raw water.

2. Methodology

2.1. Selected DWTPs, sampling and bulk analysis

Sample handling was performed using glass containers and stored in dark refrigerators at 4 °C. The routine DWTP measurements of TOC, conductivity, turbidity, pH, and ion chromatography concentrations were performed for each sample according to standard protocols (Table SI 1). Three different DWTPs managed by the same company (Ens d'Abastament d'Aigua Ter-Llobregat, ATL) were selected for this study to compare possible dissimilarities according to their differences in water sources and treatment train configurations. Llobregat DWTP (PTL) sources raw water from the Llobregat River and has a treatment capacity of 3.2 $m^3 \cdot s^{-1}$, supplying water to the metropolitan area of Barcelona. Due to the presence of salt deposit mining activities in the upper part of the river basin, high salinity issues are common, particularly concerning bromide concentrations. Consequently, an electrodialysis reversal (EDR) desalination operation is usually included in the treatment train (full-scale), as depicted in Fig. 1. The water is directly diverted from the river and subjected to pre-oxidation with potassium permanganate, followed by coagulation/flocculation and filtration through sand and activated carbon filters. The flow is then split into the EDR at a percentage depending on the specific requirements and on the water quality parameters (Valero and Arbós, 2010), which during the sample campaign was 64 %. Finally, the treated water is disinfected with sodium hypochlorite before being stored in tanks (Godo-Pla et al., 2021, 2019).

Also, waters from reservoirs were collected from the Ter DWTP (PTT) and Cardener DWTP (PTC). PTT takes water from a system of water reservoirs connected in series (Sau-Susqueda-Pasteral) of the Ter River through a 56-km pipeline with a maximum treatment capacity of 8 m^3/s (Postigo et al., 2018). PTC has a treatment capacity of 0.35 m^3/s of water coming from the Llosa del Cavall reservoir.

Bench-scale (BS) studies were conducted to test the removal efficiency of anion exchange resin (IEX) LEWATIT® S5128 (PWNT, Holland) by taking samples before (BS-1) and after (BS-2) the coagulation process. The resin was conditioned by repeatedly washing with MilliQ water until the absorbance at 254 nm (A254) was <0.2 $abs \cdot m^{-1}$. Then, 0.40 mL of resin was added to each litre of the sample, and the mixture was agitated at 120 rpm for 30 min. Notably, bench-scale studies were conducted focusing solely on the performance of IEX aiming to study in which point this technology would be more efficient to improve the treatment capacity of the plants in removing specific fractions of organic matter and its potential impact on THMFP.

After the IEX testing (BS-1), the catchment samples were subjected to coagulation/flocculation jar testing using PAX-XL10 (25 $mg \cdot L^{-1}$) (Kemira, Finland) and PoliDADMAC Magnafloc LT7992 (0.8 $mg \cdot L^{-1}$) (Solenis, USA) as coagulant and flocculant, respectively.

2.2. DOM fractionation (HPSEC-DAD-OCD)

DOM fractionation was studied using a chromatographic system (HPSEC-DAD-OCD). The methodology was optimized from previous SEC methods (Huber et al., 2011) to obtain higher chromatographic resolutions, mainly achieved by the combination of two SEC columns in series. Size exclusion separation was performed using an Agilent 1260 Infinity II HPLC (Agilent Technologies, USA) with a 1260 vial sampler coupled to a DAD, enabling UV detection during the whole sweep from 200 to 400 nm. The chromatograph was hyphenated to a Sievers M9 SEC OCD operating in turbo mode (data acquisition every 4 s). Full methodological parameters are detailed in previous work (Valenti et al., 2022).

Five main DOM fractions were identified from the HPSEC-DAD-OCD chromatograms, with retention times (R_t) according to their apparent MW: biopolymers (MW > 10 kDa, R_t 10.8–16 min), humic substances (HS, 10 kDa > MW > 700 Da; R_t 16–22.5 min), building blocks (BB, 700 Da > MW > 200 Da; R_t 22.5–29 min), low molecular weight acids (MW < 200 Da; R_t 29–33 min), and low molecular weight neutrals (MW < 200 Da; R_t 33–60 min).

To analyse the HS sub-fractions, we calculated the specific UV absorbance (SUVA) profiles of the three particular peaks: HS1, 19.2 min;

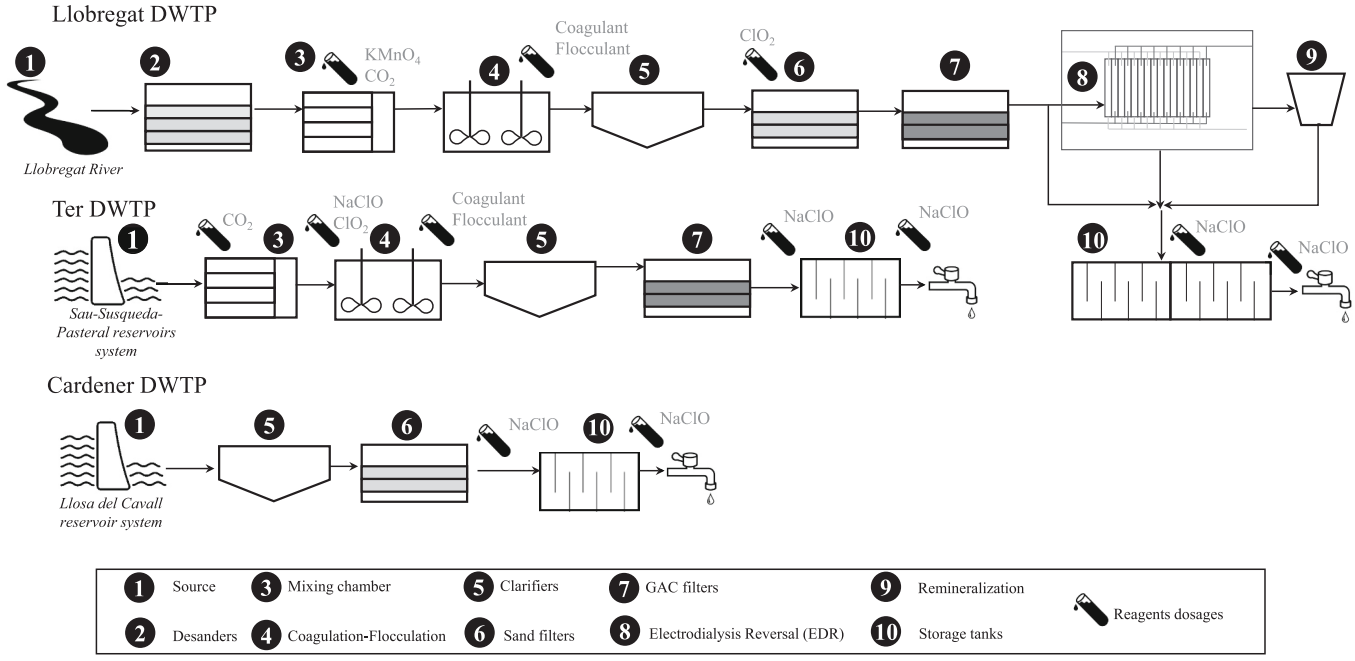

Fig. 1. Scheme of the full-scale treatment trains and points of reagents addition at the Llobregat (PTL), Ter (PTT) and Cardener (PTC) drinking water treatment plants.

HS2, 20.1 min; HS3, 20.45 min. The full spectra raging 200 to 400 nm was divided for the DOC at the specific elution time corresponding to humic substances sub-fractions.

2.3. Trihalomethane formation potential analysis

The formation potential of regulated trihalomethanes (THMFP) - trichloromethane (TCM, CHCl3), bromodichloromethane (BDCM, CHBrCl2), dibromochloromethane (DBCM, CHBr2Cl), tribromomethane (TBM, CHBr3) - and total THM (TTHM), calculated as the sum of the four species, was determined following the standard procedures (Standard Method 5710 A). The analysis was conducted using headspace chromatography with electron capture detection (HS-GC-ECD) after 72 h of reaction time. Certified disinfectants, confirmed to be free of bromide contamination, were used for all tests to ensure accurate measurement of brominated THM formation.

3. Results and discussion

3.1. DOM characterization of source and treated waters

HPSEC-DAD-OCD constitutes an advanced tool for probing the compositional changes within DOM fractions, offering useful insights for treatment optimization (Huber et al., 2011). Differences in UV absorbance profiles and DOC concentration among DOM fractions across the diverse water sources and DWTP treatment highlight the heterogeneous nature of DOM composition. Overall, the variations in water quality parameters between river and reservoir sources have implications for subsequent treatment processes and water quality management. To comparatively assess the efficiency of the treatment trains, an initial analysis of source and final treated water was performed.

3.1.1. Treatment plants from river sources: PTL

Starting with the bulk water quality parameters (Table 1), PTL, which sources water from the Llobregat River, the TOC concentration is 3.17 $mg{\cdot}L^{-1}$, indicating a moderate level of organic carbon content. The UV absorbance at 254 nm (A_{254}) was 5.98 UA (Units of Absorbance), suggesting a significant presence of organic matter with absorbance properties and a high turbidity at 23.00 NTU. This water has a high concentration of ions, particularly Br^-, NO_3^- and SO_4^{2-}, which concentrations were 0.55 $mg{\cdot}L^{-1}$, 4.10 $mg{\cdot}L^{-1}$ and 123.78 $mg{\cdot}L^{-1}$, respectively.

Differences in distributions and intrinsic characteristics of DOM fractions were qualitatively evaluated using HPSEC-DAD-OCD analysis through the overlap of the SEC chromatograms, encompassing both DOC and UV-absorption spectra (Fig. 2).

PTL water catchment presented the greatest prevalence of DOM fractions in the range of 10 kDa to 200 Da. This corresponds to humic substances (HS, 16 min–24 min) and building blocks (BB, 24 min–29 min), accounting for 40.9 % and 39.2 % of DOC respectively (Table 2). Additionally, 4.1 % of the DOC corresponded to biopolymers (R_t 10.8 min–16 min), a notably higher value compared to the other studied plants, which treat waters from reservoirs.

The absorbance of HS spanned nearly the entire UV range (200 nm – 400 nm) with moderate intensity. However, the BB fraction exhibited the strongest signal intensity from 200 nm to 230 nm (R_t 22.5 min to 27 min). However, it must be noted that the ions contained in PTL samples are removed through HPSEC separation from all DOM fractions except those within the BB region, where inorganic ions co-elute (R_t 23.2 min and 25 min) (Valenti et al., 2022). Thus, in this specific region, the UV profiles at lower wavelengths (< 220 nm) may not solely reflect the properties of DOM but also residual ions (Ignatev and Tuhkanen, 2019; Korshin et al., 1997).

After the full treatment, as shown in Fig. 2B, the absorbance decreased due to the removal of chromophoric compounds, combined with a reduction in DOC of the predominant HS fraction. This resulted in a decrease in the signal intensity and in the narrowing of the absorption wavelength ranges up to 325 nm. Also, bromide, nitrate, and sulphate were reduced up to 0.18 $mg{\cdot}L^{-1}$, 2.17 $mg{\cdot}L^{-1}$, and 49,48 $mg{\cdot}L^{-1}$ respectively in the effluent sample.

3.1.2. Treatment plants from reservoir sources: PTT and PTC

For PTT catchment, the TOC bulk concentration was 2.92 $mg{\cdot}L^{-1}$, and the A_{254} value was 6.61 UA, indicating a comparable level of organic carbon content and absorbance properties to PTL. Turbidity was lower at 0.85 NTU, suggesting less suspended particles compared to PTL.

According to the DOM fraction analysis, HS constituting the 48.9 % of the DOM fractions, with BB representing the 33.7 % of the DOC (Table 2). The source of PTT had lower levels of nitrate (1.91 $mg{\cdot}L^{-1}$), sulphate (10.87 $mg{\cdot}L^{-1}$), and undetectable levels of bromide. However, it presented the highest intensities among all samples, both in the influent and effluent (Fig. 2, A2–B2).

Regarding the PTT effluent (Fig. 2, B2), the final concentrations of main absorbing fractions, especially BB, still accounted for high intensity, suggesting minimal removal of those most highly absorbing chromophores. However, the spectral range narrowed, shifting towards lower wavelengths.

Similarly, the water quality parameters in the PTC catchment were within a comparable range. The bulk TOC concentration was 1.38 $mg{\cdot}L^{-1}$, indicating a lower level of organic carbon compared to PTL and

Table 1
Bulk water parameters of the samples across treatment operations in the three Treatment Plants (TP) evaluated.

DWTP	Sample	TOC [$mg{\cdot}L^{-1}$]	A_{254} [UA]	SUVA [$ua{\cdot}L{\cdot}mg^{-1}$]	Conductivity [$\mu S{\cdot}cm^{-1}$]	Turbidity [NTU]	pH	Br^- [$mg{\cdot}L^{-1}$]	NO_3^- [$mg{\cdot}L^{-1}$]	SO_4^{2-} [$mg{\cdot}L^{-1}$]
PTL	Catchment	3.17	5.98	1.89	1186	23.00	8.07	0.55	4.10	123.78
Full Scale	C/F	2.57	4.65	1.81	1204	0.33	7.72	0.56	3.71	123.59
	Adsorption	1.74	2.73	1.57	1212	0.48	7.64	0.56	4.68	123.58
	EDR	1.22	1.37	1.12	345	0.28	6.91	0.10	0.98	27.30
	Chlorination	1.49	2.43	1.64	647	0.28	7.91	0.18	2.17	49.48
PTL	IEX (BS-1)	1.83	1.52	0.83	1295	14.1	8.04	0.09	0.85	3.65
BS	C/F (BS-1)	1.99	2.91	1.46	1293	2.3	7.68	<LOQ	0.92	20.06
	IEX (BS-2)	1.64	1.15	0.70	1298	0.37	7.71	0.09	0.76	3.93
PTT	Catchment	2.92	6.61	2.26	392	0.85	8.08	<LOQ	1.91	10.87
Full Scale	C/F	2.51	4.21	1.68	382	0.27	7.72	0.15	5.30	29.03
	Adsorption	2.00	2.74	1.37	376	0.35	7.77	0.12	4.03	21.89
	Chlorination	1.86	2.82	1.51	396	0.21	7.84	<LOQ	3.92	18.88
PTT	IEX (BS-1)	1.32	1.04	0.79	460	0.70	8.02	<LOQ	0.60	1.64
BS	C/F (BS-1)	2.53	1.39	0.55	458	0.64	7.69	0.02	0.67	20.16
	IEX (BS-2)	1.02	0.79	0.77	461	0.37	7.75	<LOQ	0.47	1.67
PTC	Catchment	1.38	2.51	1.82	568	0.60	8.09	<LOQ	0.98	79.99
	C/F	1.30	2.42	1.86	568	0.33	8.11	<LOQ	0.99	80.52
	Chlorination	1.27	1.49	1.17	572	0.15	8.11	<LOQ	0.82	62.26

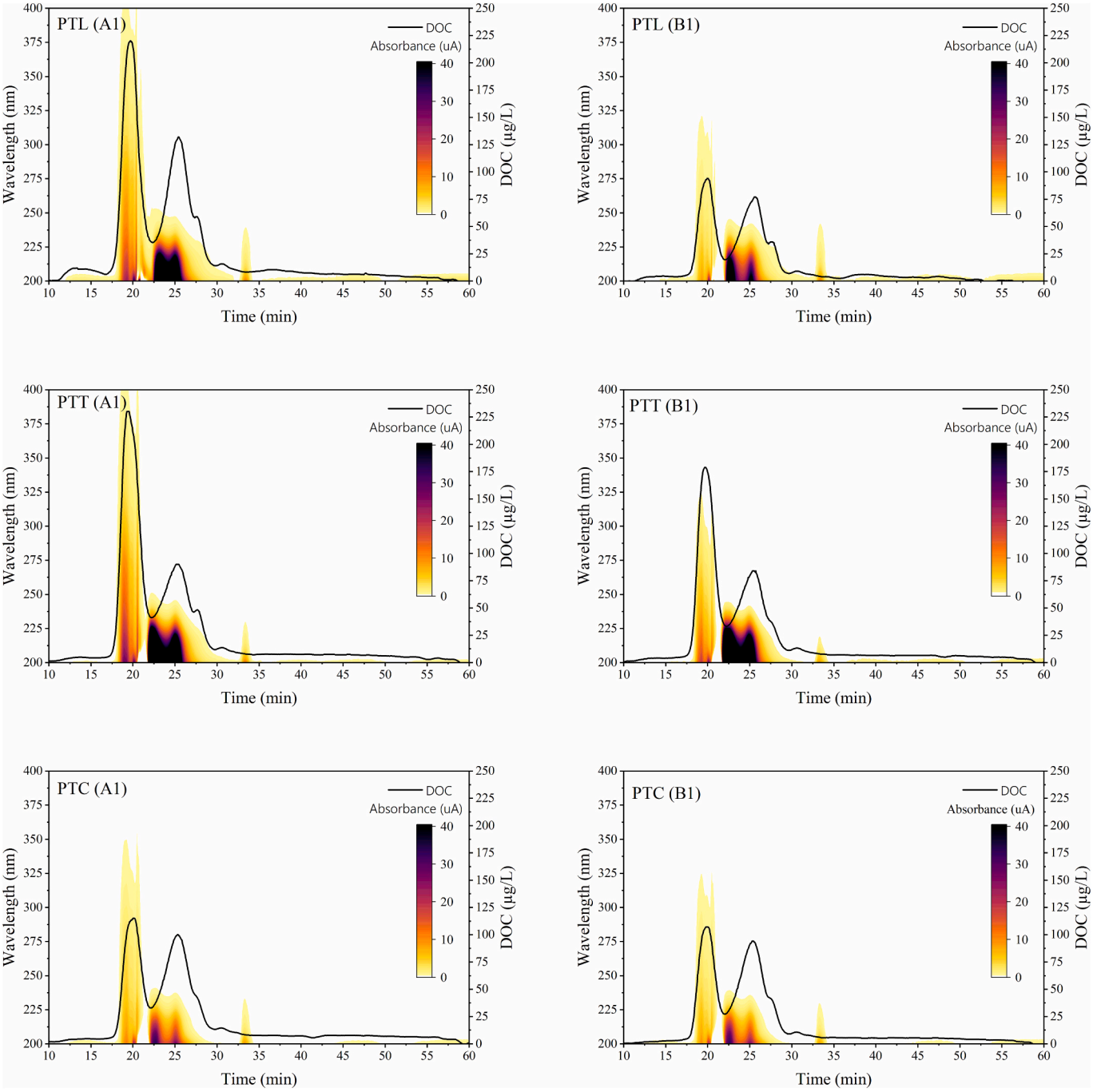

Fig. 2. Overlapped DOC and UV-multiwavelength absorbance profiles from HPSEC chromatograms of catchments (A1–3) and treated waters (B1–3) after conventional treatment train (R_t 10.8–16 min: Biopolymers; R_t 16–22.5 min: HS; R_t 22.5–29 min: BB; R_t 29–33 min: low MW acids; R_t 33–60 min: low MW neutrals).

PTT. A_{254} was 2.51 UA and turbidity was 0.60 NTU, suggesting a moderate presence of organic matter compared to PTL. PTC had the lowest amounts of inorganic ions (0.98 $mg{\cdot}L^{-1}$ NO_3^-, 79.99 $mg{\cdot}L^{-1}$; SO_4^{2-}, and undetectable concentrations of Br^-).

However, the DOM presented a completely distinct distribution profile, characterized by lower amount of HS corresponding to 30.5 % of DOC, and higher percentage of BB corresponding to the 46.4 %. Similarly, compared to the other catchment samples, lower quantities of chromophoric compounds were detected in these samples (Fig. 2, A3). Also, PTC showed the least DOC removal (7 %) within the treatment train (Fig. 2, B3), with scarce variations in the maximum wavelength absorption (from 325 nm to 350 nm) of the chromophores associated with the HS.

When comparing HPSEC elution times, which are indicative of the molecular weight of the DOM fractions, peak maximums of HS and BB in PTT exhibited higher values compared to those in PTL and PTC. Specifically, in PTT, the R_t for HS and BB were 19.3 min and 25.6 min, respectively, while in PTL, they were 19.8 min for HS and 25.2 min for BB. Similarly, in PTC, the elution times were 20.1 min for HS and 25.3 min for BB.

3.2. *Sequential removal of DOM fractions*

Upon analysing samples from the operational works, each DOM fraction exhibited different responses after undergoing the water treatment operations. All HPSEC chromatograms can be seen in Supporting

Table 2
Distribution of DOC in DOM fractions by HPSEC-DAD-DOC.

DWTP	Sample	BioP [%]	HS [%]	BB [%]	LMW acids [%]	LMW neutrals [%]
PTL	Catchment	4.1	40.9	39.2	3.4	12.3
Full	C/F	3.0	34.7	44.3	4.3	13.7
Scale	Adsorption	1.6	31.2	50.5	4.1	12.6
	EDR	2.5	31.2	47.8	3.4	15.2
	Chlorination	2.8	37.8	44.8	3.6	11.0
PTL	IEX (BS-1)	7.0	22.1	46.3	4.9	19.7
BS	C/F (BS-1)	3.4	32.8	26.6	11.6	25.6
	IEX (BS-2)	5.5	21.7	43.7	6.0	23.1
PTT	Catchment	1.9	48.9	33.7	3.3	12.2
Full	C/F	1.5	47.6	35.8	3.3	11.7
Scale	Adsorption	1.6	41.6	42.1	2.7	12.0
	Chlorination	2.2	43.9	36.4	3.6	13.9
PTT	IEX (BS-1)	3.1	30.9	31.9	9.5	24.6
BS	C/F (BS-1)	2.4	36.7	18.3	11.3	31.4
	IEX (BS-2)	3.8	29.2	29.9	10.6	26.5
PTC	Catchment	2.3	30.5	46.4	4.3	16.5
	C/F	2.3	29.7	48.5	4.2	15.4
	Chlorination	1.8	32.2	49.5	3.4	13.1

information (Figs. SI 1–4). To facilitate the visualization of precise changes, Fig. 3 presents the reduction in each DOC fraction concentration (μg/L) after each successive treatment operation calculated by subtracting the concentration measured before and after the operation.

3.2.1. Full scale DWTPs

Coagulation, as a physicochemical process performed in the three DWTPs studied, affects the repulsive potential of the electrical charge and hydrophobicity of DOM constituents, facilitating their aggregation into microparticles and turbidity removal. The variation in DOM nature and the operational conditions among DWTPs lead to variations in the efficiency of the process. Coagulation accounted for a significant removal of HS fraction in the full-scale treatment configuration, being comparatively lower in the reservoir waters PTT (60 μg/L) and PTC (26 μg/L) than in PTL (109 μg/L) as presented in Fig. 3. Notably, there was no reduction in the BB fraction DOC concentration after coagulation in any of the DWTPs, while biopolymers experienced a slight decrease, which was expected given their high molecular weight. This results in changes in the DOC distribution across the different DOM fractions after coagulation in the three DWTPs evaluated, reducing proportion of HS and increasing BB (Table 2).

PTL and PTT supplied with GAC adsorption after coagulation operation unit. Unlike coagulation, GAC targets the HS of lower molecular weight and lower aromaticity, and the BB fractions. In PTL, a HS reduction of 50 μg/L was achieved, while in PTT the reduction reached 126 μg/L. In PTL, a DOC increase was detected in the BB fraction (−50 μg/L), suggesting the possibility of organic material release from the activity of the filters.

The EDR, as part of the full-scale treatment in PTL, reported significant DOC reductions in the BB fraction of 221 μg/L. While the inorganic ions elute at the same R_t as BB in the HPSEC separation, they do not contribute to the DOC signal. Consequently, the observed differences in DOC are attributed to DOM removal.

The final disinfection stage entailed variations primarily in BB for both PTL and PTT DWTPs, as measured by the DOC detector. However, no significant effect was produced over PTC. Chlorination reactions might consume that specific DOM fraction, leading to the formation of DBPs, including THM.

3.2.2. IEX bench-scale

Ion exchange (IEX) performance was evaluated in bench scale in both PTL and PTT. Two configurations were considered in each case: IEX applied to the catchment water followed by a coagulation process (BS-1), and the reverse order, IEX applied after the full-scale coagulation operation (BS-2). The order and combination of processes involving IEX

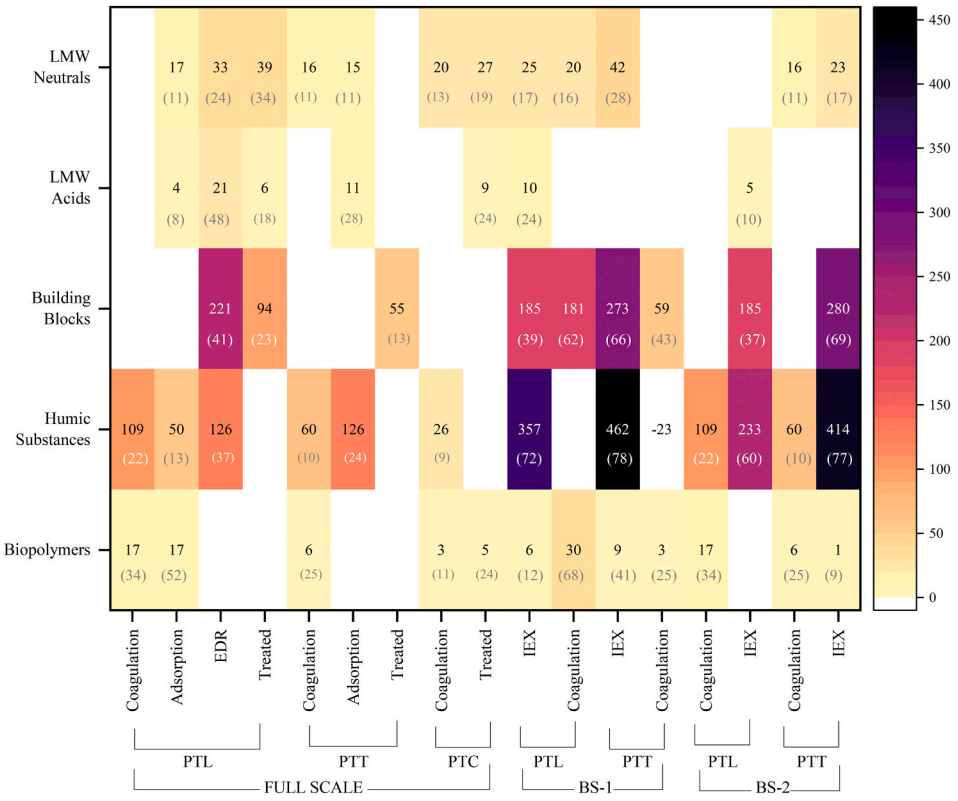

Fig. 3. Differences in the concentration of DOC (μg/L) for each DOM fraction after treatments, calculated by subtracting subsequent concentrations. The intensity of colours represents the magnitude of differences, with more intense colours indicating higher decrease of DOC. Values in brackets express the reduction %.

may play a significant role in the performance, since the treatment decreases the charge density of the water, thereby facilitating the removal of higher hydrophilic compounds during the subsequent coagulation processes (Andersson et al., 2020; Finkbeiner et al., 2020; Tan and Kilduff, 2007).

In PTL the removal of HS achieved in a single IEX process (357 μg/L) surpassed the combined removal achieved by coagulation, adsorption and EDR in full scale. This increase was even more pronounced in PTT, where IEX achieved a HS removal of 462 μg/L. Using the configuration BS-2, the efficiency of HS removal was decreased, since a significant part of this fraction was previously removed by coagulation in the full-scale, leading to the same overall HS reduction in both configurations for both DWTPs.

On the contrary, there was a significant difference in the removal efficiency of the BB fraction depending on the BS configuration for both DWTPs. In PTL, IEX achieves a removal of 185 μg/L of BB regardless of the configuration. However, post-IEX coagulation achieved an additional 181 μg/L that was not removed before IEX. Similarly, in PTT, coagulation before IEX did not result in any BB removal, while IEX removed approximately 280 μg/L in both configurations, with an additional 59 μg/L removal after coagulation.

Throughout all treatments, including full and bench-scale processes, it was observed that LMW compounds, including both acids and neutrals, exhibited high recalcitrance. In particular, acids showed minimal alterations, and the most noticeable changes were observed in the removal of neutrals after processes involving ion removal such and IEX. Therefore, following BS treatments there is a noticeable shift in the distribution of DOC across DOM fractions (Table 2).

3.3. Humic substances sub-fractions

In light of water characterization, HS are identified as the most abundant fraction constituting DOM in the studied source waters, displaying diverse removal efficiencies across treatment operations. This section focuses on assessing the performance of both full-scale treatment processes and bench-scale IEX technologies, with particular attention to the predominant HS sub-fractions. The alterations in BB sub-fractions were lesser compared to those of the HS, yet slight significant variations were observed, suggesting that lower MW DOM fractions, with certain aromaticity, may play a role as THM precursor.

Biopolymers, including protein-like compounds, were excluded from this study due to their low concentrations relative to the total DOM (ranging between 2 and 4 %, see Table 2) in the analysed source waters. Furthermore, these compounds were effectively removed during early

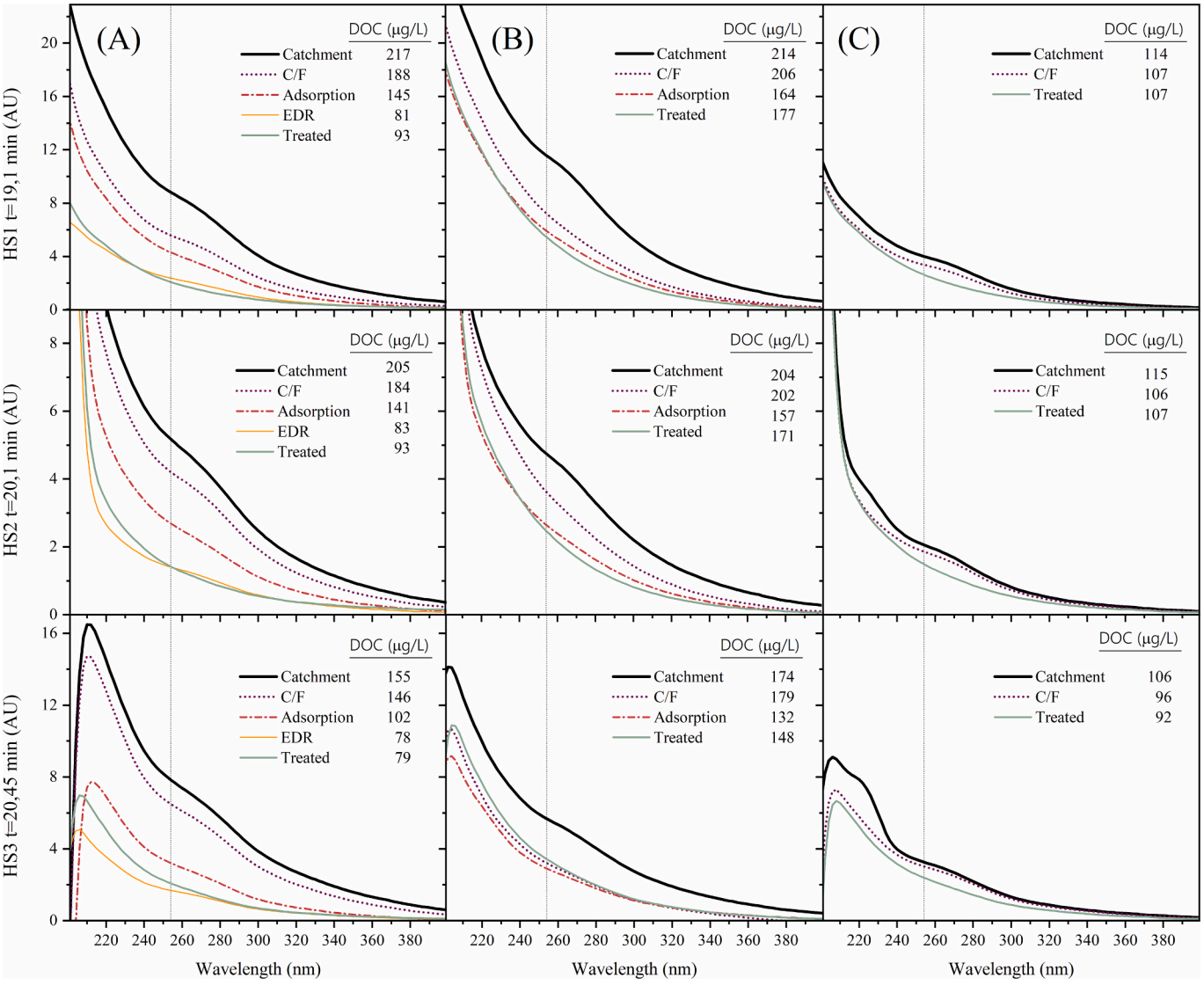

Fig. 4. Overlap of absorbance spectra from Humic Substances peaks (HS1, HS2, HS3) of (A) PTL, (B) PTT and (C) PTC full scale treatment train. Vertical lines mark 254 nm.

stages of the conventional treatment process, such as coagulation and adsorption (see Fig. 3). Therefore, we determined that this fraction did not warrant further evaluation as a THMFP precursor in this specific study.

3.3.1. UV-multiwavelength analysis of humic substances sub-fractions

A more profound analysis of divergences between HS sub-fractions was performed by evaluating their full absorbance profile Fig. 4 shows the spectroscopic profile in UV absorbance spectra (200 nm to 400 nm) within the humic substances HS1, HS2 and HS3 after each treatment unit. By considering the full absorbance spectra rather than single-wavelength monitoring, the sensitivity of the analysis is enhanced, allowing for a more accurate determination of the relationships between DOM fractions and DBPs formation (Helms et al., 2008).

The absorbance profiles of both HS1 and HS2 were similar in PTL and PTT, despite the different source of these DWTPs. PTC presented a lower profile, particularly in HS1 and HS3 than the other plants, which was consistent with the bulk values previously observed (Table 1). Across the three waters evaluated, there was a peak in the absorbance profile of each HS sub-fractions around 270 nm, with higher intensity in PTT compared to PTL and PTC. This wavelength has been widely associated to aromatic groups related to DBP formation (Korshin et al., 2009).

Further differences were observed in adsorption features, with additional absorbance peaks around 250 nm, and 270 nm, revealing the presence of benzene adsorption bands (Brezinski and Gorczyca, 2019). Moreover, a shoulder near 280 nm is observed in both PTL and PTT, while electronic transitions $\pi \rightarrow \pi^*$ from benzene rings bound to double C = O are denoted with an absorbance maximum at 310 nm (Chen et al., 2020). These transitions are typical of oxidation products acting as DBP precursors. Regarding HS3, an adsorption peak around 230 nm suggests the presence of carboxylic and aromatic chromophores (Korshin et al., 2009).

Throughout the treatment processes, spectroscopic changes are observed particularly in the range between 240 nm and 310 nm. The variations noted in HS2 sub-fraction in PTT were minor than in HS1, where the intensity of the signal dropped significantly, particularly at lower wavelengths (200–240 nm).

The relationship between the differential absorbance at 272 nm and its correlation with THM has been extensively studied (Zhang et al., 2021, 2020). In PTT, after coagulation, this absorbance maximum was smoothed out for all three subfractions, indicating the early depletion of these chromophores during the initial stages of treatment. However, a distinct behavior was observed in PTL, where this maximum disappeared only after the late treatments of EDR and disinfection. The phenolic compounds present in the HS undergo electrophilic aromatic substitution reactions with chlorine (Criquet et al., 2015). These reactions affect fast chromophores, which are more reactive and are primarily consumed during the initial stages of chlorination, such as carboxylic and aromatic groups, which absorb at wavelengths below 250 nm. Subsequently, the formation of cyclic and tautomeric ketones, hydroquinones, and catechols may occur, with absorption peaks above 250 nm, encompassing the reactivity of slower chromophores like activated aromatic groups (Chen et al., 2020). This mechanism is associated with the reactivity of the low MW phenols via two-electron oxidation reaction and is considered the main pathway for DBP formation (Wenk et al., 2013). Finally, it is worth noting that the effect of halogenation at higher wavelength (λ >350 nm) is spectroscopically negligible (Byrne et al., 2011). Although the absorbance variation in that range after chlorination processes should be genuinely characteristic of DOM constituents, it was not observed in our findings.

The absorbance ratios at specific wavelengths have been linked with DOM properties such as aromaticity (A_{210}/A_{254}), polarity (A_{220}/A_{254}) or proportion between autochthonous and terrestrial DOM (A_{254}/A_{436}) (Cascone et al., 2022; Ignatev and Tuhkanen, 2019). The calculation of these ratios for the different HS sub-fractions provides deeper insights into the composition of these substances (Table 3).

In terms of aromaticity and polarity, PTT accounted for the highest levels, reflected in the lowest A_{210}/A_{254} and A_{220}/A_{254} ratio, followed by PTL and PTC. Specifically, HS1 was the most aromatic polar fraction, while HS2 presented the lowest aromaticity, and HS3 exhibited the least polar properties. The highest A_{254}/A_{436} ratios were observed for PTC and PTT, suggesting more terrestrial characteristics, as expected for reservoir waters in comparison with PTL. Across all samples, higher molecular weight HS sub-fractions showed the highest A_{254}/A_{436} ratios (HS1 > HS2 > HS3). The variability was more pronounced in PTC, where both HS1 and HS2 were similar as PTT. In contract, PTL exhibited similarities between HS2 and HS3, the lowest MW humics.

3.3.2. Evaluating the removal of humic substances

To assess a comprehensive evaluation of the diverse humic substances composition, Fig. 5 depicts the distributions of DOC, and $SUVA_{254}$ within the HS sub-fraction at the three given retention times (HS1, 19.1 min; HS2, 20.1 min; and HS3, 20.45 min). The excluded portion of the fraction mainly gathers the lower weight tail of the peak, referred to as HS_{LMW}.

The DOC quantification of HS sub-fractions revealed that HS1, the sub-fraction of higher apparent MW, was the most abundant across all water samples, a proportion that was maintained during both conventional and advanced treatments. Regarding aromaticity, HS1 also exhibited the highest absorbance at 254 nm compared to HS2 and HS3 in general terms. The evaluation of the treatment operations across the DWTPs revealed varied responses to HS sub-fractions removal, emphasizing the complex dynamics or DOM removal.

Coagulation mainly reduced chromophores in the HS fractions of higher molecular weight and aromaticity: HS1. The A_{254} was reduced by 42 %, 45 % and 21 % and the DOC concentration in 26 %, 19 % and 8 % for PTL, PTT, and PTC respectively. These findings sustain the selectivity of coagulation-flocculation processes on removing compounds of HMW and hydrophobicity. Overall, the impact of coagulation-flocculation on HS removal suggests that DOM chromophores were predominantly of a higher nucleophilic nature. Notably, absorbance differences in HS were most pronounced between 200 nm and 240 nm, with steeper slopes compared to higher wavelength regions (i.e., 360 nm to 400 nm), where absorbances remained relatively consistent across treatments (Fig. 4).

Moreover, the comparison of the A_{210}/A_{254} ratio highlights differences in the composition after coagulation, with PTT showed a higher proportion of aliphatic HS fractions compared to PTL. This contributes to the sustained reduction of performance in the subsequent adsorption processes. Contrasting observations in PTC, where differences in $SUVA_{254}$ were evident but DOC removals of HS fractions were nearly equal, suggest that short wavelength chromophores removal may arise predominantly from coagulation.

GAC filtration targeted fractions of lower apparent MW, i.e., HS2, HS3, and HS_{LMW}, resulting in DOC removal efficiencies ranging from 21 to 26 % in both TPs. However, the corresponding decrease in A_{254} was much more pronounced in PTL compared to PTT, as evidenced in Fig. 4. Adsorption removal is enhanced by electrostatic forces, thus the diverse susceptibilities of the DOM fractions to the treatment. Low MW HS are

Table 3
Absorbance ratios of humic substances fraction of catchment samples.

DWTP	Ratio	HS1 (19.1 min)	HS2 (20.1 min)	HS3 (20.45 min)
PTL	210/254	2.1	2.6	2.1
PTT		1.9	2.3	2.2
PTC		2.1	2.9	2.7
PTL	220/254	1.7	1.8	1.8
PTT		1.6	1.7	1.8
PTC		1.7	1.9	2.4
PTL	254/436	15.8	14.9	14.1
PTT		18.8	18.3	14.5
PTC		24.6	21.5	18.9

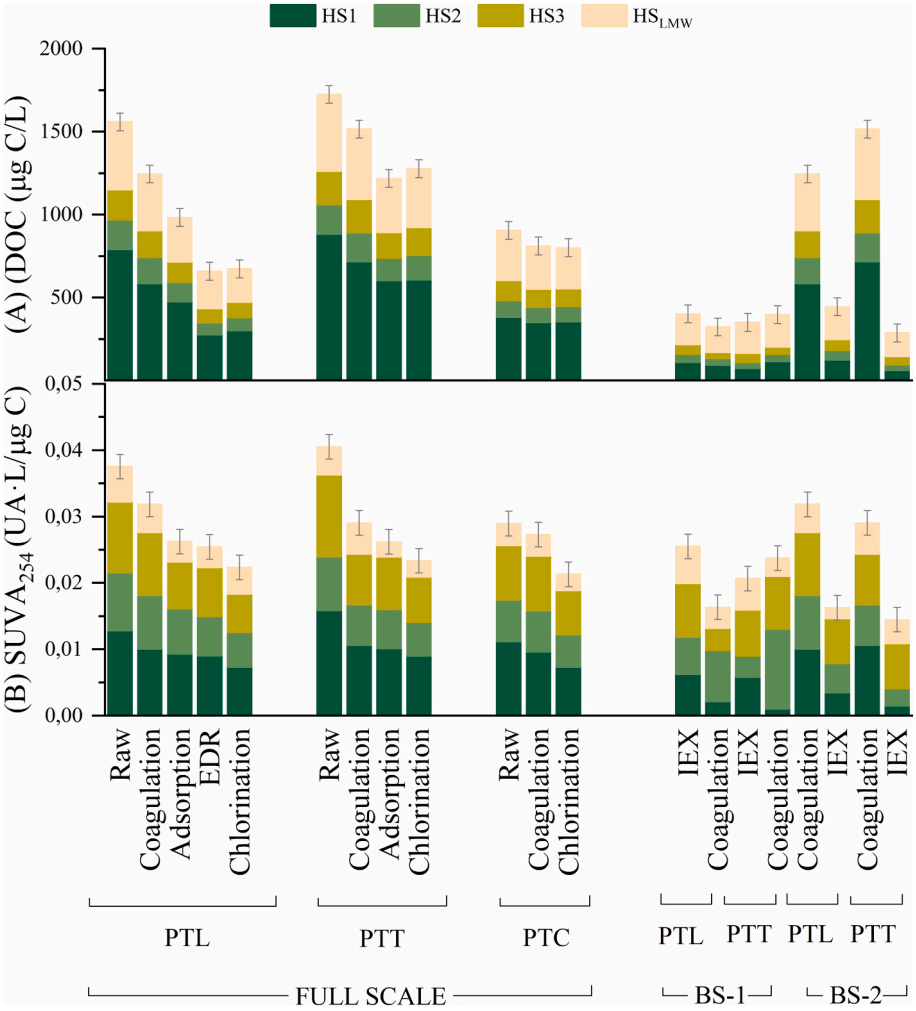

Fig. 5. Distribution of humic substances fractions according to (A) DOC and (B) SUVA254 analysis of HS1, HS2, HS3 and HS_{LMW} in full scale DWTP and bench-scale advanced treatments in PTL, PTT and PTC.

richer in saturated moieties of less hydrophobicity, yet they are polar enough to be prone to adsorption removal. However, except from adsorption, low MW fractions remained recalcitrant in other conventional treatments, turning them into precursors for DBPs formation.

Although EDR mainly targets the removal of anions, it still leads to a significant decrease in aromatic compounds, especially those of higher molecular weight in HS1 and HS2, with DOC removal of 24 % and 19 % respectively.

Ion-exchange accounted for the highest removals both in terms of concentration and absorbance over the conventional treatments (>80 %). Specially targeting fractions of higher molecular weight (HS1), yet HS2, HS3, and HS_{LMW} where largely removed (>50 %) compared to other treatments. Those findings suggest that ion exchange could be a suitable technology for compounds containing ionized groups such as carboxylic and phenolic groups, electron-rich structures of high molecular weight which abundant in HS.

The detailed analysis of SUVA254 revealed its utility as a surrogate parameter assessing DOM characteristics, despite its limitations when analysed alone. SUVA254 focuses on changes on aromatic HS fractions, which behaved differently during treatment processes, and DOC and A254 alone might not capture these subtle variations (Fig. 5B). SUVA254 indicated similar reactivity for HS1 and HS3 across conventional treatments, it was able to detect an increase in aromaticity for HS2 following coagulation and ion-exchange treatments.

3.4. Assessment of THMFP through conventional and IEX treatments

3.4.1. THMFP in treatment plants from river sources: PTL

In PTL, the initial THMFP (72 h) of the catchment water before treatment showed concentrations of 38.8 µg/L of TCM, 108.6 µg/L of BDCM, 134.5 µg/L of DBCM and 70.1 µg/L of TBM. This distribution reflects the bromide concentration of the catchment water (Table 1). Fig. 6 illustrates the reduction on the THMFP achieved after each operation during the water treatment processes, for each specie and for the total, referred as TTHM.

Coagulation was found to be the most effective operation for reducing TTHMFP in PTL, primarily targeting the reduction of BDCMFP and DBCMFP. Additionally, after adsorption, further reductions in TTHMFP were observed, influenced by the alterations on the DOM fractions distribution (Fig. 3) that affected particularly HS of lower MW (Fig. 5), causing a decrease of DBCM. The application of EDR resulted in a significant alteration in their reactivity, enhancing the removal of bromide, and consequently the FP of brominated THM (TBM and DBCM). After completing the whole treatment train process, there was a reduction of 73 % in TTHMFP, with concentrations of 4.2 µg/L for TCMFP, and 24.5 µg/L for DBCMFP.

In the bench-scale IEX testing, combining IEX and coagulation led to more pronounced reductions in THMFP. The order and combination of processes played a significant role in the speciation of THM, with IEX treatment decreasing the charge density of the water and facilitating the removal of higher hydrophilic compounds during subsequent

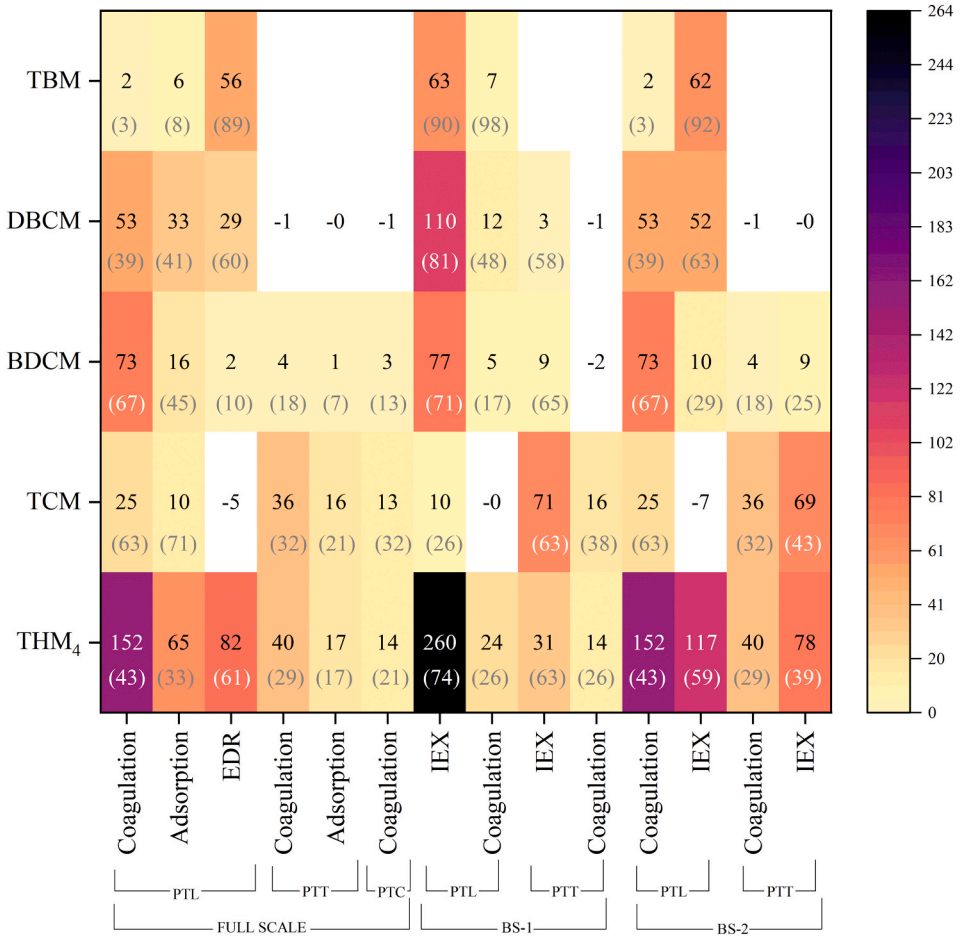

Fig. 6. Reduction in THM formation potential (THMFP) shown as differences between unitary operations in full-scale treatments and bench-scale IEX tests (BS-1, BS-2) for each DWTP. The values are presented in μg/L, with colours indicating the magnitude of THM-FP reduction: darker colours represent greater reductions. Values in brackets express the reduction %.

coagulation processes (Andersson et al., 2020; Finkbeiner et al., 2018). The overall decrease in the FP of brominated THM achieved in bench scale was higher than in conventional full scale.

3.4.2. *THMFP in treatment plants from reservoir sources*

In contrast to PTL, PTT had undetectable levels of bromide (Table 1), leading to a different profile of brominated DBPs. In catchment water the most abundant species were TCM (87.6 μg/L), followed by BDCM (20.1 μg/L) and DBCM (2.8 μg/L), with undetectable levels of TBM. Consequently, the total initial TTHMFP was half of PTL.

Coagulation was effective in reducing TTHMFP in PTT, primarily targeting the reduction of TCM. Additionally, after adsorption processes, there were slight reductions in TTHMFP in PTT. However, the effects were less pronounced compared to PTL. After completing the entire treatment process, there was a reduction of 39 % in TTHMFP. Likewise, in bench-scale IEX testing, the reductions in TTHMFP were less significant in PTT compared to PTL.

Similar to PTT, PTC also had undetectable levels of bromide. The initial TTHMFP was 49.1 μg/L, distributed as 27.5 μg/L of TCM, 15.3 μg/L of BDCM and 6.4 μg/L of DBCM. Coagulation was effective in reducing TTHMFP, primarily targeting the reduction of the dominant specie, TCM, achieving a reduction of 27 % in TTHMFP.

3.5. *Assessment of humic substances and THMFP correlation*

Most treatment processes target HS, whose changes can be tracked using DOC, absorbance measurements, and other surrogate parameters. HS are crucial in THM formation due to their high molecular weight, aromaticity, and hydrophobic nature, which make them reactive towards chlorine (Chowdhury et al., 2010; Westerhoff et al., 2004). This section examines how changes in HS, as measured by DOC, A_{254}, and $SUVA_{254}$, impact THMFP. Pearson correlation analysis was used to explore these relationships, with results shown in Fig. 7. Due to bromide's influence on THM speciation in PTL river water, results are analysed separately for PTL and reservoir waters.

In PTL, significant correlations (p-value ≤ 0.05) were found between DOC and A_{254} with the total TTHMFP for HS1 and HS2. These correlations were particularly strong for brominated THMs (BDCM and TBM), indicating that HS1 and HS2 are closely linked to the formation of these THMs. However, no significant correlation was observed for HS3, and TCM and BDCM FP did not correlate with any HS parameters in PTL.

In contrast, reservoir water demonstrated a different pattern. TCM-PF showed a clear correlation with the A_{254} of the three HS sub-fractions. However, this spectroscopic correlation did not extend in terms of DOC. Overall, the A_{254} of the major sub-fraction HS1 exhibited a strong correlation with the TTHMFP. Thus, the observed differences between PTL and reservoir waters can be attributed to:

i) the DOM Composition: Reservoir waters, particularly PTT, have higher aromaticity than PTL's river water, as indicated by higher SUVA values. This increased aromaticity is linked to greater conjugation (e.g., double bonds and carboxylic groups), which enhances the reactivity of DOM with chlorine, leading strong correlations between A_{254} of HS sub-fractions and THMFP in reservoir waters.

ii) the presence of Bromide: High bromide levels in PTL river water

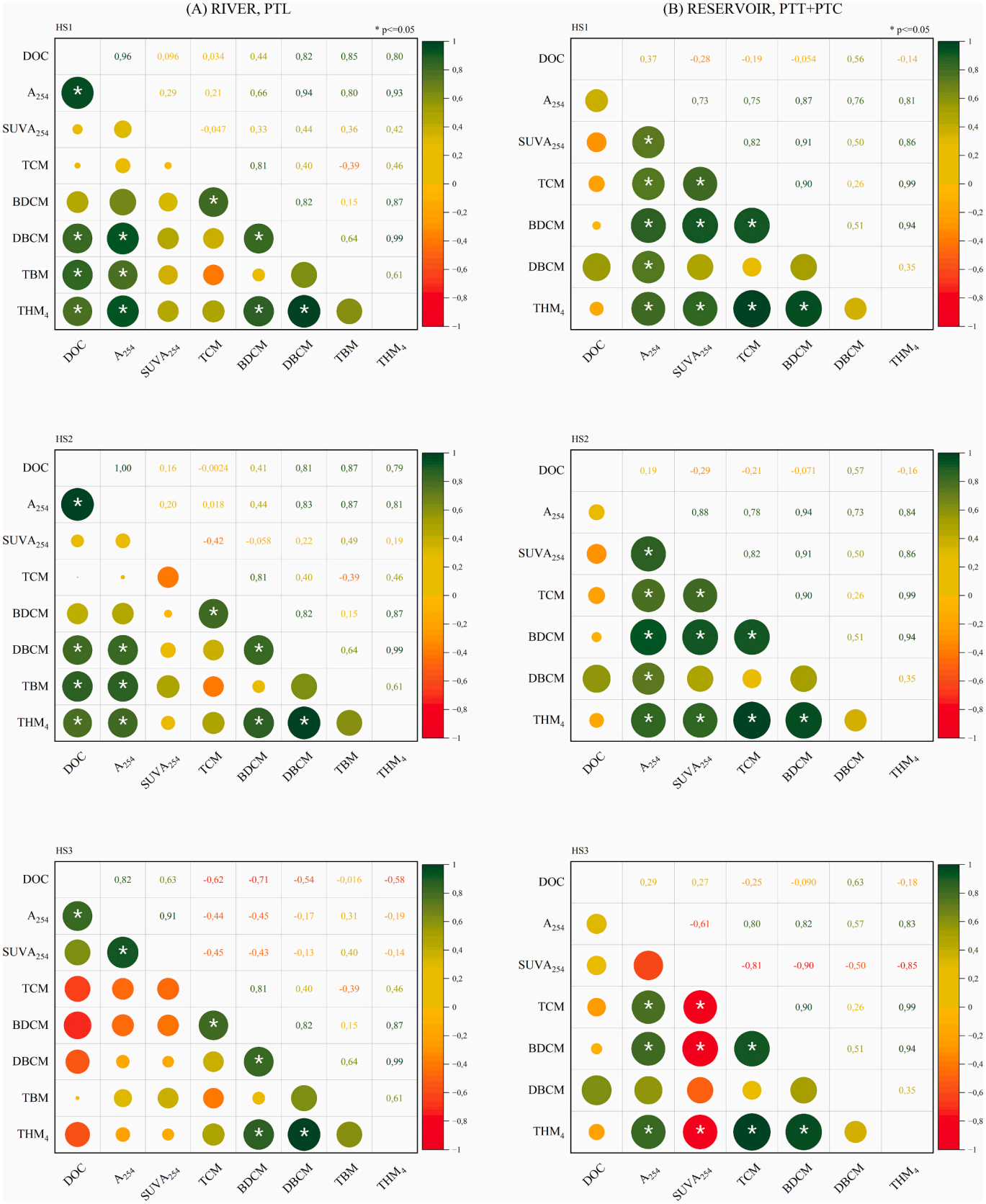

Fig. 7. Pearson's correlation matrices of HS surrogate parameters and THMFP. Significant correlations (p-value ≤0.05) are marked with * symbol. Column A: River, Column B: Reservoir.

lead to lower formation of TCM and extended formation of BDCM and TBM, which correlate differently with HS sub-fractions. Thus, river waters show different correlation patterns, reflecting clearer relationships between DOC of HS1 and HS2 and brominated THM-FP.

Overall, these findings suggest that detailed spectroscopic analysis of DOM provides valuable insights into its role in DBP formation. This is consistent with (Awad et al., 2016), who found that monitoring general parameters like DOC alone may not fully capture DOM reactivity towards DBP formation in the presence of bromide.

4. Conclusions

The application of HPSEC-DAD-OCD enabled a detailed analysis of the absorbance profiles of DOM fractions and HS sub-fractions, shedding light on their role as DBP precursors. The analysis revealed differences in DOM composition, highlighting the heterogeneity within the samples and providing insights into their reactivity as THM precursors. By evaluating the full absorbance profile of HS sub-fractions, the study achieved enhanced sensitivity and accuracy in determining the relationships between DOM fractions and THMFP. This comprehensive approach provides a deeper understanding of how different treatments impact these fractions.

Conventional water treatment processes, such as coagulation and GAC adsorption, mainly targeted higher MW DOM fractions, while EDR and IEX were more effective for the removal of lower MW fractions, including building blocks and LMW compounds, which often remained recalcitrant to standard treatments. Treatment processes significantly altered the absorbance profiles, particularly in the 240–310 nm range. Coagulation, for instance, effectively reduced chromophores in higher molecular weight and aromatic HS fractions, indicating its selectivity in removing such compounds. In contrast, GAC filtration targeted lower molecular weight fractions, with varied efficiency across DWTPs.

The DOC quantification revealed that HS1, the ones of higher MW, was the most abundant and aromatic sub-fraction across all samples. The varied responses of HS sub-fractions to different treatments underscored the complex dynamics of DOM removal. Coagulation showed significant reductions in higher molecular weight and aromaticity fractions, while GAC filtration and ion-exchange treatments were more effective for lower molecular weight fractions.

Spectroscopic analysis provided valuable insights into DOM functionalities, supporting the differentiation of reactivity between samples, compared to unspecific measurements like DOC. This approach not only reinforced the importance of characterizing waters but also emphasized the site-specificity of treatment requirements, enabling more efficient treatment tailoring.

The absorbance profiles of HS1 and HS2 (high and mid MW HS) in PTL and PTT were similar, despite originating from different sources. However, PTC exhibited a lower profile, particularly in HS1 and HS3 (lowest MW), aligning with previously observed bulk values. All three water sources showed a peak around 270 nm, associated with aromatic groups linked to DBP formation. This peak was most intense in PTT, suggesting a higher presence of DBP precursors. Additional peaks and shoulders in the absorbance spectra further indicated the presence of benzene adsorption bands and oxidation products, which are typical DBP precursors.

The absorbance ratios at specific wavelengths (A_{210}/A_{254}, A_{220}/A_{254}, A_{254}/A_{436}) provided insights into the aromaticity, polarity, and source characteristics of DOM. For instance, PTT showed the highest aromaticity and polarity, while PTC indicated more terrestrial characteristics. These ratios also helped identify the composition and reactivity of different HS sub-fractions based on their physicochemical properties.

River-sourced water exhibited distinct THM speciation compared to reservoir-sourced water, influenced by the presence of bromide. Significant correlations between surrogate parameters and TTHMFP for specific HS sub-fractions elucidate the link between DOM characteristics and THM formation potentials. In river-sourced water, brominated THM species showed clear correlations with both DOC and A_{254} of HS1 and HS2, while in reservoir-sourced water, A_{254} of major HS sub-fractions exhibited strong correlations with TTHMFP.

Despite the comprehensive analysis, challenges remain in fully understanding the interactions between DOM fractions and treatment processes. Future studies should continue to refine the use of surrogate parameters, especially spectroscopic, and explore advanced analytical techniques to better predict DBP formation potential and optimize treatment strategies.

CRediT authorship contribution statement

Meritxell Valenti-Quiroga: Writing – review & editing, Writing – original draft, Visualization, Methodology, Investigation, Formal analysis, Data curation, Conceptualization. **Alba Cabrera-Codony:** Writing – review & editing, Visualization. **Pere Emiliano:** Resources. **Fernando Valero:** Resources. **Hèctor Monclús:** Funding acquisition. **Maria J. Martin:** Writing – review & editing, Visualization, Supervision, Project administration.

Declaration of competing interest

The authors declare that they have no known competing financial interests or personal relationships that could have appeared to influence the work reported in this paper.

Data availability

Data will be made available on request.

Acknowledgements

This study was supported by the WATSproof (CTM2017-83598-R) and ShERLOcK projects (PID2020-112615RA-I00), financed by the Ministerio de Ciencia e Innovación (Spain). MVQ thanks AGAUR from the Generalitat de Catalunya for a predoctoral grant under the program FI_SDUR 2020-00330. LEQUIA has been recognised as a consolidated research group by the Catalan government (2017-SGR-1552). Open access funding was provided thanks to the CRUE-CSIC agreement with Elsevier.

Appendix A. Supplementary data

Supplementary data to this article can be found online at https://doi.org/10.1016/j.scitotenv.2024.176600.

References

Abouleish, M.Y.Z., Wells, M.J.M., 2015. Trihalomethane formation potential of aquatic and terrestrial fulvic and humic acids: sorption on activated carbon. Sci. Total Environ. 521–522, 293–304. https://doi.org/10.1016/j.scitotenv.2015.03.090.

Andersson, A., Lavonen, E., Harir, M., Gonsior, M., Hertkorn, N., Schmitt-Kopplin, P., Kylin, H., Bastviken, D., 2020. Selective removal of natural organic matter during drinking water production changes the composition of disinfection by-products. Environ Sci (Camb) 6, 779–794. https://doi.org/10.1039/C9EW00931K.

Awad, J., van Leeuwen, J., Chow, C., Drikas, M., Smernik, R.J., Chittleborough, D.J., Bestland, E., 2016. Characterization of dissolved organic matter for prediction of trihalomethane formation potential in surface and sub-surface waters. J. Hazard. Mater. 308, 430–439. https://doi.org/10.1016/j.jhazmat.2016.01.030.

Bhatnagar, A., Sillanpää, M., 2017. Removal of natural organic matter (NOM) and its constituents from water by adsorption – a review. Chemosphere 166, 497–510. https://doi.org/10.1016/j.chemosphere.2016.09.098.

Bond, T., Henriet, O., Goslan, E.H., Parsons, S.A., Jefferson, B., 2009. Disinfection byproduct formation and fractionation behavior of natural organic matter surrogates. Environ. Sci. Technol. 43, 5982–5989. https://doi.org/10.1021/es900686p.

Brezinski, K., Gorczyca, B., 2019. Multi-spectral characterization of natural organic matter (NOM) from Manitoba surface waters using high performance size exclusion chromatography (HPSEC). Chemosphere 225, 53–64. https://doi.org/10.1016/j.chemosphere.2019.02.176.

Byrne, A.J., Chow, C., Trolio, R., Lethorn, A., Lucas, J., Korshin, G. V., 2011. Development and validation of online surrogate parameters for water quality monitoring at a conventional water treatment plant using a UV absorbance spectrolyser, in: Proceedings of the 2011 7th International Conference on Intelligent Sensors, Sensor Networks and Information Processing, ISSNIP 2011. pp. 200–204. doi:https://doi.org/10.1109/ISSNIP.2011.6146515.

Carra, I., Fernandez Lozano, J., Johannesen, S., Godart-Brown, M., Goslan, E.H., Jarvis, P., Judd, S., 2021. Sorptive removal of disinfection by-product precursors from UK lowland surface waters: impact of molecular weight and bromide. Sci. Total Environ. 754, 142152. https://doi.org/10.1016/j.scitotenv.2020.142152.

Cascone, C., Murphy, K.R., Markensten, H., Kern, J.S., Schleich, C., Keucken, A., Köhler, S.J., 2022. AbspectroscoPY, a Python toolbox for absorbance-based sensor data in water quality monitoring. Environ Sci (Camb) 8, 836–848. https://doi.org/10.1039/D1EW00416F.

Chen, B., Zhang, C., Zhao, Y., Wang, D., Korshin, G.V., Ni, J., Yan, M., 2020. Interpreting main features of the differential absorbance spectra of chlorinated natural organic matter: comparison of the experimental and theoretical spectra of model compounds. Water Res. 185, 116206. https://doi.org/10.1016/j.watres.2020.116206.

Chen, W., Yu, H.-Q., 2021. Advances in the characterization and monitoring of natural organic matter using spectroscopic approaches. Water Res. 190, 116759. https://doi.org/10.1016/j.watres.2020.116759.

Chowdhury, S., Champagne, P., James McLellan, P., 2010. Investigating effects of bromide ions on trihalomethanes and developing model for predicting bromodichloromethane in drinking water. Water Res. 44, 2349–2359. https://doi.org/10.1016/j.watres.2009.12.042.

Criquet, J., Rodriguez, E.M., Allard, S., Wellauer, S., Salhi, E., Joll, C.A., von Gunten, U., 2015. Reaction of bromine and chlorine with phenolic compounds and natural organic matter extracts – electrophilic aromatic substitution and oxidation. Water Res. 85, 476–486. https://doi.org/10.1016/j.watres.2015.08.051.

Drikas, M., Dixon, M., Morran, J., 2011. Long term case study of MIEX pre-treatment in drinking water; understanding NOM removal. Water Res. 45, 1539–1548. https://doi.org/10.1016/j.watres.2010.11.024.

Finkbeiner, P., Redman, J., Patriarca, V., Moore, G., Jefferson, B., Jarvis, P., 2018. Understanding the potential for selective natural organic matter removal by ion exchange. Water Res. 146, 256–263. https://doi.org/10.1016/j.watres.2018.09.042.

Finkbeiner, P., Moore, G., Pereira, R., Jefferson, B., Jarvis, P., 2020. The combined influence of hydrophobicity, charge and molecular weight on natural organic matter removal by ion exchange and coagulation. Chemosphere 238, 124633. https://doi.org/10.1016/j.chemosphere.2019.124633.

Gibert, O., Lefèvre, B., Fernández, M., Bernat, X., Paraira, M., Pons, M., 2013. Fractionation and removal of dissolved organic carbon in a full-scale granular activated carbon filter used for drinking water production. Water Res. 47, 2821–2829. https://doi.org/10.1016/j.watres.2013.02.028.

Godo-Pla, L., Emiliano, P., Valero, F., Poch, M., Sin, G., Monclús, H., 2019. Predicting the oxidant demand in full-scale drinking water treatment using an artificial neural network: uncertainty and sensitivity analysis. Process Saf. Environ. Prot. 125, 317–327. https://doi.org/10.1016/j.psep.2019.03.017.

Godo-Pla, L., Emiliano, P., Poch, M., Valero, F., Monclús, H., 2021. Benchmarking empirical models for THMs formation in drinking water systems: an application for decision support in Barcelona. Spain. Science of The Total Environment 763, 144197. https://doi.org/10.1016/j.scitotenv.2020.144197.

Helms, J.R., Stubbins, A., Ritchie, J.D., Minor, E.C., Kieber, D.J., Mopper, K., 2008. Absorption spectral slopes and slope ratios as indicators of molecular weight, source, and photobleaching of chromophoric dissolved organic matter. Limnol. Oceanogr. 53, 955–969. https://doi.org/10.4319/lo.2008.53.3.0955.

Huber, S.A., Balz, A., Abert, M., Pronk, W., 2011. Characterisation of aquatic humic and non-humic matter with size-exclusion chromatography - organic carbon detection - organic nitrogen detection (LC-OCD-OND). Water Res. 45, 879–885. https://doi.org/10.1016/j.watres.2010.09.023.

Ignatev, A., Tuhkanen, T., 2019. Step-by-step analysis of drinking water treatment trains using size-exclusion chromatography to fingerprint and track protein-like and humic/fulvic-like fractions of dissolved organic matter. Environ Sci (Camb) 5, 1568–1581. https://doi.org/10.1039/C9EW00340A.

Korshin, G., Chow, C.W.K., Fabris, R., Drikas, M., 2009. Absorbance spectroscopy-based examination of effects of coagulation on the reactivity of fractions of natural organic matter with varying apparent molecular weights. Water Res. 43, 1541–1548. https://doi.org/10.1016/j.watres.2008.12.041.

Korshin, G.V., Li, C.-W., Benjamin, M.M., 1997. Monitoring the properties of natural organic matter through UV spectroscopy: a consistent theory. Wat. Res 31, 1787–1795.

Korshin, G.V., Wu, W.W., Benjamin, M.M., Hemingway, O., 2002. Correlations between differential absorbance and the formation of individual DBPs. Water Res. 36, 3273–3282. https://doi.org/10.1016/S0043-1354(02)00042-8.

Peacock, M., Evans, C.D., Fenner, N., Freeman, C., Gough, R., Jones, T.G., Lebron, I., 2014. UV-visible absorbance spectroscopy as a proxy for peatland dissolved organic carbon (DOC) quantity and quality: considerations on wavelength and absorbance degradation. Environ Sci Process Impacts 16, 1445. https://doi.org/10.1039/c4em00108g.

Postigo, C., Emiliano, P., Barceló, D., Valero, F., 2018. Chemical characterization and relative toxicity assessment of disinfection byproduct mixtures in a large drinking water supply network. J. Hazard. Mater. 359, 166–173. https://doi.org/10.1016/j.jhazmat.2018.07.022.

Roccaro, P., Vagliasindi, F.G.A., Korshin, G.V., 2009. Changes in NOM fluorescence caused by chlorination and their associations with disinfection by-products formation. Environ. Sci. Technol. 43, 724–729. https://doi.org/10.1021/es801939f.

Rodríguez, F.J., Schlenger, P., García-Valverde, M., 2016. Monitoring changes in the structure and properties of humic substances following ozonation using UV–vis, FTIR and 1 H NMR techniques. Sci. Total Environ. 541, 623–637. https://doi.org/10.1016/j.scitotenv.2015.09.127.

Shi, Z., Chow, C.W.K., Fabris, R., Liu, J., Jin, B., 2022. Applications of online UV-vis spectrophotometer for drinking water quality monitoring and process control: a review. Sensors 22, 2987. https://doi.org/10.3390/s22082987.

Tan, Y., Kilduff, J.E., 2007. Factors affecting selectivity during dissolved organic matter removal by anion-exchange resins. Water Res. 41, 4211–4221. https://doi.org/10.1016/j.watres.2007.05.050.

Valenti-Quiroga, M., Daunis-i-Estadella, P., Emiliano, P., Valero, F., Martin, M.J., 2022. NOM fractionation by HPSEC-DAD-OCD for predicting trihalomethane disinfection by-product formation potential in full-scale drinking water treatment plants. Water Res. 227, 119314. https://doi.org/10.1016/j.watres.2022.119314.

Valero, F., Arbós, R., 2010. Desalination of brackish river water using Electrodialysis Reversal (EDR). Control of the THMs formation in the Barcelona (NE Spain) area. Desalination 253, 170–174. https://doi.org/10.1016/j.desal.2009.11.011.

Valverde, A., Cabrera-Codony, A., Calvo-Schwarzwalder, M., Myers, T.G., 2024. Investigating the impact of adsorbent particle size on column adsorption kinetics through a mathematical model. Int. J. Heat Mass Transf. 218, 124724. https://doi.org/10.1016/j.ijheatmasstransfer.2023.124724.

Velten, S., Knappe, D.R.U., Traber, J., Kaiser, H.-P., von Gunten, U., Boller, M., Meylan, S., 2011. Characterization of natural organic matter adsorption in granular activated carbon adsorbers. Water Res. 45, 3951–3959. https://doi.org/10.1016/j.watres.2011.04.047.

Wang, G.-S., Hsieh, S.-T., 2001. Monitoring natural organic matter in water with scanning spectrophotometer. Environ. Int. 26, 205–212. https://doi.org/10.1016/S0160-4120(00)00107-0.

Wenk, J., Aeschbacher, M., Salhi, E., Canonica, S., von Gunten, U., Sander, M., 2013. Chemical oxidation of dissolved organic matter by chlorine dioxide, chlorine, and ozone: effects on its optical and antioxidant properties. Environ. Sci. Technol. 47, 11147–11156. https://doi.org/10.1021/es402516b.

Westerhoff, P., Chao, P., Mash, H., 2004. Reactivity of natural organic matter with aqueous chlorine and bromine. Water Res. 38, 1502–1513. https://doi.org/10.1016/j.watres.2003.12.014.

Yan, M., Korshin, G., Wang, D., Cai, Z., 2012. Characterization of dissolved organic matter using high-performance liquid chromatography (HPLC)–size exclusion chromatography (SEC) with a multiple wavelength absorbance detector. Chemosphere 87, 879–885. https://doi.org/10.1016/j.chemosphere.2012.01.029.

Zhang, C., Chen, B., Korshin, G.V., Kuznetsov, A.M., Roccaro, P., Yan, M., Ni, J., 2020. Comparison of the yields of mono-, Di- and tri-chlorinated HAAs and THMs in chlorination and chloramination based on experimental and quantum-chemical data. Water Res. 169. https://doi.org/10.1016/j.watres.2019.115100.

Zhang, C., Roccaro, P., Yan, M., Korshin, G.V., 2021. Interpretation of the formation of unstable halogen-containing disinfection by-products based on the differential absorbance spectroscopy approach. Chemosphere 268. https://doi.org/10.1016/j.chemosphere.2020.129241.